High negative ion production yield in 30 keV F2++ adenine (C5H5N5) collisions

B Li, X Ma, X L Zhu, S F Zhang, H P Liu, W T Feng, D B Qian, D C Zhang, L Chen, R Brédy, et al.

J. Phys. B: At. Mol. Opt. Phys. **42** (2009) 075204 (5pp) doi:10.1088/0953-4075/42/7/075204

High negative ion production yield in 30 keV F^{2+} + adenine ($C_5H_5N_5$) collisions

B Li[1,2,3], X Ma[1], X L Zhu[1], S F Zhang[1,2], H P Liu[1], W T Feng[1,2], D B Qian[1], D C Zhang[1], L Chen[3], R Brédy[3], G Montagne[3], J Bernard[3] and S Martin[3]

[1] Institute of Modern Physics, Chinese Academy of Sciences, Lanzhou 730000, People's Republic of China
[2] Graduate University of Chinese Academy of Sciences, Beijing 100049, People's Republic of China
[3] Université de Lyon, F-69622, Lyon, France; Université Lyon 1, Villeurbanne; CNRS, UMR5579, LASIM

E-mail: chen@univ-lyon1.fr

Received 17 November 2008, in final form 27 January 2009
Published 20 March 2009
Online at stacks.iop.org/JPhysB/42/075204

Abstract
In collisions between slow F^{2+} ions (30 keV) and molecular targets, adenine, scattered particle production yields have been measured directly by simultaneous detection of neutrals, positive and negative ions. The relative cross-section for a negative ion formation channel was measured to be 1%. Despite a slight decrease compared to a larger target, the fullerene C_{60}, the measured negative ion formation cross section is still at least one order of magnitude larger than the yield in ion–atom interactions.

1. Introduction

In collisions between slow ions ($v < 1$ a.u.) and atoms, molecules, clusters or surfaces, the scattered negative ions can be considered as a probe for studying the target properties [1]. One of the applications of negative ion analysis has been demonstrated by the so-called double charge transfer spectroscopy by measuring the double ionization potential of small diatomic molecules [2–4]. In H^+–molecule collisions, Furuhashi *et al* have measured the energy loss of scattered negative H^- ions using a high-resolution kinetic energy spectrometer with a resolution up to 0.15 eV [4]. This resolution was sufficient to resolve vibrational levels of the excited molecular states. A similar method, called collision induced dissociation under energy control (CIDEC), has been developed in the recent past years to study the fragmentation of the fullerene C_{60} [5, 6]. In H^+–C_{60} collisions, by analysing the kinetic energy loss of the scattered negative projectile ion H^-, the internal energy distribution of the doubly charged C_{60} has been obtained for the main dissociation channels, i.e. the successive evaporation of C_2 units [5]. This experiment shows that the production of negative ions provides an opportunity for measuring the energy deposited in a complex isolated target before its further dissociation.

The negative ion production yield depends sensitively on the properties of the target (dimension, structure, ionization potentials, etc). Using atomic or diatomic targets, this production yield has never exceeded 0.1% [2]. The largest negative ion production yield up to 60%–90% has been observed in grazing collisions of ions on a LiF surface target, where a large number (from 20 to 70) of binary collision sequences with F^- lattice sites were implied [7, 8]. For isolated targets, as in the case of fullerene C_{60}, the intermediate negative-ion-production-rate has been reported with projectile ions at low initial charge states. For example, with F^{q+} ($q = 1$, 2, 3) at $v = 0.18$ a.u., the yield has been measured to be 7%, 3% and 1%, respectively [9]. These values are much larger than in the cases of atomic targets. Such unexpected high negative ion production yields for a target with a limited size were interpreted as due to multi-electron capture to the ground state of the projectile in grazing collisions where the projectile passes in the electronic cloud of the C_{60} cage.

Compared to C_{60} and atoms or diatomic molecules, a DNA building block like the adenine is a target of intermediate size. The interaction between slow ions and such small molecules and their clusters has attracted increasing interests during the last few years [10–14]. From these pioneer works, new questions have been raised concerning the dynamics of the damages induced by the slow secondary ions created

along the track of the primary beams in radiotherapy. To study the dissociation mechanism of molecular targets, the excitation energy deposited by ion impact is a determinant parameter. To measure precisely the energy deposited in the targets, the CIDEC method could be a good approach provided that the negative ion production yield is high enough in collisions between a slow ion beam and the targets. The first application of the CIDEC method to small molecules of biological relevance has been performed recently for adenine [15] and deoxyribose [16], while the negative ion formation dynamics in collisions with such small fragile molecules is still not well understood.

The aim of this work is to investigate this problem by measuring the negative ion production yield in collisions between F^{2+} ions at keV energy range and one of the base molecules of DNA, adenine. In the following, the negative ion production rate γ^- is defined as the ratio $\sigma^-/\sigma_{\text{total}}$ between the F^- production cross section over the total charge exchange cross section. The total cross section, $\sigma_{\text{total}} = \sigma^- + \sigma^0 + \sigma^+$, includes the contributions of negative, neutral and positive scattered projectiles F^-, F^0 and F^+. In the present low collision energy range, electron capture is the dominant process. The relative cross section of a direct ionization and excitation channel leading to F^{2+} scattered ions is estimated to be less than 10^{-2}. Therefore, this channel will be neglected and scattered F^{2+} will not be discussed in the following. To analyse the final charge state of scattered projectiles, an electrostatic analyser is often employed [17]. Such a device can provide high-resolution measurement in kinetic energy analysis of the ions, however it prevents one from measuring the neutralized particles under identical experimental conditions. In a previous work in Lyon, a multicoincidence technique [9] has been employed to determine the negative ion production yield using the C_{60} target. However, this method is only suitable for targets that could remain intact (non-fragmented) after the collision but not for more fragile targets such as molecules of DNA bases, which undergo multifragmentation in general after a primary negative ion production channel [15]. The development of an alternative method is therefore necessary.

In the present work, we report an experimental method for measuring directly the production yield of all scattered projectiles. The scattered positive, neutral and negative particles were separated by an electrostatic deflector and measured simultaneously by a position sensitive detector. The detection of the scattered projectiles was performed in coincidence with the time-of-flight (TOF) spectrum of the recoil ions to exclude contributions of charge exchange in collisions with residual gas in the beam transport line.

2. Experiment

A schematic view of the experimental setup is shown in figure 1. The projectile ions F^{2+} at 2×15 keV were delivered by the ECR ion source of the Institute of Modern Physics in Lanzhou. The ions, selected in mass over charge, entered in the experimental line after a 45° magnet. The beam was then collimated by two sets of four-jaw slits separated by a distance of 800 mm (not shown in the sketch). Before entering the collision chamber, the primary beam was selected by a 30° coaxial cylindrical electrostatic deflector. This deflector, named beam cleaner, was used to eliminate secondary beams produced by collisions of ions with residual gas during the beam transport. It has a radius of 200 mm along the ion beam trajectory and an exit slit of width 0.2 mm. In the collision chamber, the beam intersected a gas-phase adenine jet evaporated from an oven heated at 135 °C. A plate cooled at the temperature of liquid nitrogen was mounted just above the collision region to collect the molecular jet. To ensure the crossing of the fine projectile beam and the molecular jet, two sets of electrostatic plates in horizontal and vertical planes were inserted before the interaction region to drive the beam. Downstream of the collision region, the projectile ions were deflected by a parallel-plate deflector. Scattered particles F^+, F^0 and F^- that have undergone charge exchange were detected by a two-dimensional delay-line position sensitive detector (PSD) composed of a couple of multi-channel plates (MCP) of 75 mm in diameter and a homemade delay-line anode [18]. The intense primary beam F^{2+} was collected into a Faraday cup (FC) beside the detector. For each collision event, the hitting time of the scattered projectile on the detector was recorded providing the time reference for the TOF spectrometer. The recoil ions were extracted by a homogeneous electrostatic field of 169 V cm^{-1} perpendicular to the ion beam and target jet directions. The length of the acceleration and the free drift regions of the TOF were designed to fulfil the first-order focusing condition of Wiley–Mclaren. After passing through a TOF tube of 121 mm, the recoil ions were detected by a MCP detector. To increase the detection efficiency, the front MCP was biased to −2000 V to post-accelerate the recoil ions. Considering also the extraction and acceleration regions with a total potential difference of 1.0 kV, the energy of a singly charged ion gets up to 3.0 keV when it hits the detector. The recoil ion signal was sent to a multi-stop TDC unit (LeCroy 4208) for analysing the arrival time of each ion with respect to the reference signal provided by the scattered projectile PSD detector. Up to eight fragments could be analysed in a single event. The experiments were performed in an event-by-event mode.

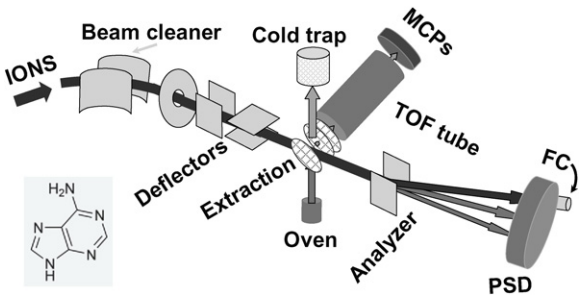

Figure 1. Experimental setup with the structure of the adenine molecule in insert.

3. Results and discussion

The image of the PSD recorded in coincidence with the detection of at least one recoil ion is presented in figure 2(a).

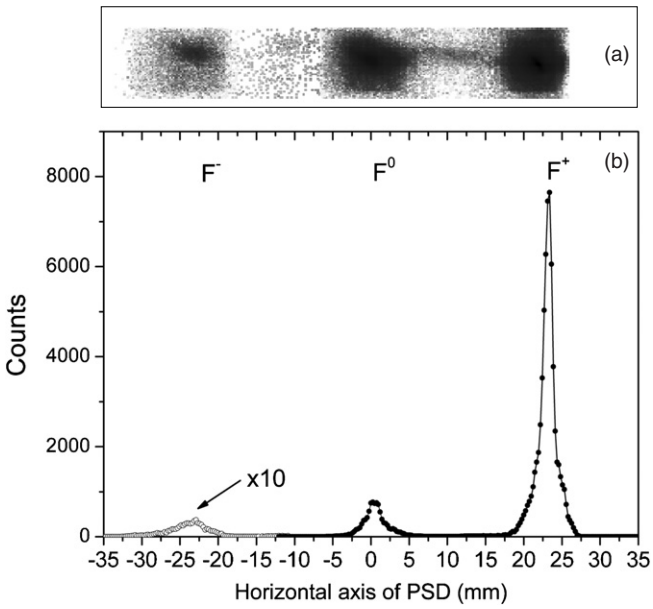

Figure 2. (a) Image of the scattered projectile particles on the position sensitive detector (PSD) measured in coincidence with the detection of at least one recoil ion with the TOF spectrometer. (b) Projection of the spectrum (a) onto the horizontal axis.

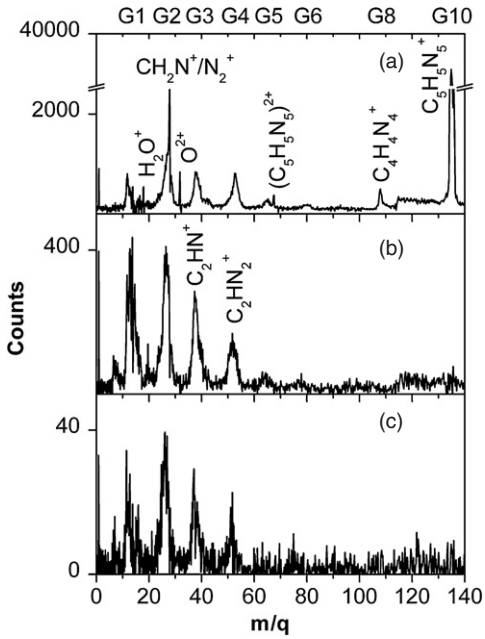

Figure 3. TOF spectra correlated to the detection of F^+ (a), F^0 (b) and F^- (c) scattered projectiles, respectively.

The spot in the centre of the detector is assigned to the neutrals F^0 that were not deflected by the parallel-plate deflector. The two lateral spots correspond respectively to the negative and positive ions F^-, F^+. Figure 2(b) presents the projection of the image onto the horizontal axis. To extract, from the experimental data, the production yield for each species of scattered particles, it is essential to consider the detection efficiency of the MCP detector for these charged and neutral particles. The absolute detection efficiency (ADE) of MCP for neutral [19] and for ionic species [20] has been studied with light and heavy atoms in the low keV energy range using methods based on coincidence techniques. It is primarily a function of the impact energy and reaches a saturated value at a critical impact energy around 3 keV [19, 20]. The comparison of the data obtained from these measurements [19, 20] shows that the ADE value for neutral atomic species is similar to that of ionic ones. In the present experiment, the impact energy of the scattered particles is about 30 keV. This is much higher than the critical energy for the ADE saturation. Therefore, it is reasonable to consider that the fluorine particles F^+, F^0 and F^- were detected by the MCP with equal efficiency.

The TOF spectra correlated to the detection of F^+, F^0 and F^- are presented in figure 3. The spectrum in figure 3(a) was recorded in coincidence with F^+. The dominant narrow peak at mass 135 corresponds to singly charged intact adenine (Ade^+ in the following) due to single electron capture from the molecule at a large impact parameter. The small narrow peak at mass 108 corresponds to $C_4H_4N_4^+ = (Ade\text{-}HCN)^+$ resulted from the emission of a HCN unit from an Ade^+ parent ion. In the following, it is sometimes convenient to assign the TOF peaks by groups denoted with the number of heavy atoms. Therefore, Ade^+ is a peak of group G10, $C_4H_4N_4^+$ is a peak of group G8. In the present experiment, the ratio between the counts of the two peaks corresponding to HCN emission and stable channels (N_{108}/N_{135}) is about 3%. Small fragments observed on this spectrum could be attributed either to the emission of several neutral fragments from singly charged parent ions Ade^+ or to the fragmentation of multiply charged adenine at higher internal energy. The appearance of both stable adenine and small fragments in the spectrum suggests that capture processes leading to the stabilization of one electron on the projectile are correlated with a broad energy distribution on the target. The energy could be as low as to keep the molecule intact and as high as to induce the breaking of the molecule to several fragments.

Adenine parent molecules at higher charge state Ade^{q+} ($q \geqslant 2$) or their fragments could contribute to the spectrum of figure 3(a), as long as the final charge state of the scattered projectile is F^+. In these cases, based on the electron number conservation rule, $q - 1$ electrons should be ejected. Therefore, the spectra related to parent ions with different charge state could be separated by using a coincidence technique that includes the detection of the number of ejected electrons [21]. Unfortunately it was not possible to implement this technique in the present experiment. The first evidence of multicharged Ade in the TOF spectrum related to F^+ (figure 3(a)) is provided by the observation of stable doubly charged adenine Ade^{2+} corresponding to the small but narrow peak at $m/q = 67.5$. The coincidence of Ade^{2+} with the detection of F^+ projectile ions is remarkable. According to the classical over barrier model [22], stable Ade^{2+} ions are mostly produced in collisions at a large impact parameter where two electrons are captured gently by the projectile, $F^{2+} + Ade \rightarrow F^0 + Ade^{2+}$. At first sight, one would rather expect to observe the peak Ade^{2+} in the spectrum of figure 3(b) recorded in coincidence with neutral projectiles. This is obviously not the case. The appearance of peak Ade^{2+} in figure 3(a) indicates that in the above charge exchange process,

two electrons are transferred into doubly excited states that decay via an autoionization process, $F^{0**} \rightarrow F^{+} + 1e^{-}$. The absence of peak Ade^{2+} in figure 3(b) demonstrates that the stabilization of both excited electrons via radiative transition is highly unlikely. More theoretical efforts would be required in order to determine the electronic states that are likely to be populated on the projectile and their branching ratios concerning decay via autoionization or radiative stabilization.

Multicharged adenine parents that decay by multifragmentation could also contribute to the spectrum of F^{+} (figure 3(a)). In fact, a part of small fragments, from H^{+} to fragments of group G4 of this spectrum, were observed in coincidence with another or several other small charged fragments (not shown here), which confirmed the charge of parent ions to be equal or larger than 2 for this population. Indeed, in a previous experiment at similar experimental conditions (collisions of F^{2+} at 36 keV on Ade) [21], it has been observed that multicharged adenine Ade^{q+} ($q \geqslant 2$) produced in interactions, $F^{2+} + Ade \rightarrow F^{+} + Ade^{q+} + (q-1)e^{-}$, decay mainly by multifragmentation.

Figures 3(b) and (c) were recorded respectively in coincidence with the detection of a neutral F^{0} and a negative projectile ion F^{-}. In these spectra, peaks of small fragments are dominant and little difference can be noted. The spectrum recorded in coincidence with F^{0} (figure 3(b)) is centred on fragments with a mass between G1 and G2, while the spectrum in figure 3(c) is centred between G2 and G3 with slightly larger mass. Although, this fragment population shift suggests that in collisions leading to F^{0} and F^{-} scattered projectiles the energy deposited in the target should be slightly different, it seems difficult to get precise information concerning the negative ion formation dynamics from these spectra. The following discussion is based on what we have learned about ion-isolated target collisions [9] using a model system with a more rigid structure, the C_{60}. In that previous experiment, $F^{q+}(q = 1, 2)$ colliding on C_{60}, we have observed remarkable different features in the fragmentation spectra for the channels of neutral F^{0} and anion F^{-} productions. Small carbon cluster fragments are observed for the neutral channel while heavy fullerene fragments are dominant for the anion channel. Furthermore, these two channels are discriminated clearly by very different amount of energy deposited in the target. For example, using projectiles F^{2+}, the excitation energy of the target was measured to be around 41 eV for the F^{-} channel and larger than the multifragmentation limit of C_{60} (80 eV [6, 23]) for the F^{0} neutrals channel. From these observations, we noted that in collisions between ions and isolated targets the condition for negative ion production was much more critical than that for the production of neutrals. Neutral scattered projectiles, related to targets with high excitation energy and to multifragmentation of C_{60}, are assigned to violent frontal collisions where the ion passes through the C_{60} cage. The measured cross-section of F^{0} correlated to the multifragmentation of the target is comparable to the geometrical section of the C_{60} cage. However, the formation of a stable anion and the measured low energy deposition in the target can be only attributed to grazing collisions where the projectiles pass through the electronic cloud of the C_{60} just outside the fullerene cage. In collisions between F^{q+} ($q = 1$, 2, 3) and C_{60} [9], the production of F^{-} is attributed to direct feeding of $q + 1$ electrons to the ground state of the anion. The measured cross section of F^{-} corresponds roughly to the surface of a ring slightly beneath the electronic cloud with a inner radius $R_c = 9.1$ a.u. and a thickness of about 0.7 a.u..

Table 1. Measured scattered projectile yields in collisions between F^{2+} and adenine and in collisions between F^{2+} and C_{60} target [9, 24].

Production yields	$\gamma(F^{+})$	$\gamma(F^{0})$	$\gamma(F^{-})$
F^{2+} (30 keV)-Ade	86%	13%	1%
F^{2+} (7 keV)-C_{60}	51.7%	45%	3.3%

In spite of the different molecular structure of adenine from C_{60}, both molecules play the role of electron donor in a collision with an incident ion. We can therefore expect some common features in the negative ion and neutral formation dynamics using these two targets. For the adenine, the first hypothesis is that stable negative ions are produced by direct multi-electron transfer to the ground state of the anions. This might be possible in grazing collisions where the ions explore regions with high electronic density. Second, in frontal collisions, when the ions pass closer to the atoms of the molecule, only neutral projectiles could probably survive. This is mainly due to the fact that in the case of anion, the loosely bound electron could be easily lost in a frontal collision leading to the production of a neutral. Compared to C_{60} with a spherical shell structure, the adenine is nearly planar. In a frontal collision, the ion passes through one atomic layer instead of two as in the case of C_{60}. In a solid target, the energy deposited during a collision is proportional to the thickness. Considering molecules and clusters as solid targets of nanometre scale, the energy deposition should be reduced roughly by a factor of two for Ade compared to targets with a shell structure. Then, the difference in excitation energy for frontal and grazing collisions is expected to be less pronounced in the case of Ade compared to C_{60}. It is therefore not surprising to find only a slight population shift in the fragmentation spectra recorded in coincidence with F^{0} and F^{-} (figures 3(b) and (c)). Furthermore, the adenine is a more fragile molecule, even in grazing collisions, the energy deposited in the target is already large enough for triggering multifragmentation of the molecule.

The above analysis of the TOF spectra ensured that the measured scattered projectiles (figure 2) were produced in the interaction region by a collision with a target adenine molecule. The production yield of the scattered projectiles at each final charge state was then obtained directly by the ratio of the count of the corresponding peak in figure 2(b) over the total count number. The negative ion production yield using F^{2+} at 30 keV colliding on the adenine target was measured to be $\gamma(F^{-}) = 1\%$. The neutral production yield was found to be 13%. These values are shown in table 1 compared to the production yields of F^{-} and F^{0} measured in collisions between F^{2+} at 7 keV with C_{60} targets, $\gamma(F^{-}) = 3\%$ [9] and $\gamma(F^{0}) = 45\%$ [24]. Considering random orientation of the molecule with respect to the projectile trajectory, the mean radius of the adenine molecule could be estimated to be about

3 a.u. leading to smaller geometrical cross section for grazing collisions and frontal collisions in the present case than in the case of C_{60}. Due to the very close first ionization potential of the two targets, Ip(Ade) = 8.7 eV, Ip(C_{60}) = 7 eV, the total electron-capture cross sections estimated using the classical over the barrier model are comparable, 2×10^{-14} cm^2 and 2.5×10^{-14} cm^2 for adenine and C_{60} targets, respectively. Then, it is relevant to compare the ratio between the F^- production yields (0.03/0.01) measured with the two targets and the ratio between the geometrical sections of grazing collisions (approximately 9/3). The smaller size of the adenine molecule is therefore in qualitative agreement with the decrease of the measured relative cross section for the negative ion formation channel.

4. Summary

In summary, simultaneous detection of all scattered projectiles including positive, neutral and negative particles using the position sensitive detector is a suitable way for measuring cross sections of different collision channels with small biomolecular targets. In collisions between F^{2+} ions and adenine molecules, the production yields of F^+, F^0 and F^- have been measured to be respectively 86%, 13% and 1%. Despite a slight decrease compared to the C_{60} target, the measured negative ion formation cross section is still much larger than the yield in ion–atom interactions. Large negative ion production yield seems to be a common feature in collisions between slow ions and molecules with a certain number of loosely bound electrons. Such molecular systems provide reservoirs of electrons for incident ions. Using singly charged projectiles, higher negative ion production yield is expected offering opportunities to study the fragmentation of small molecules under energy controlled conditions using the CIDEC method.

Acknowledgments

This work was supported by the International Collaboration Convention CNRS in France (N°21657) and the National nature Science Foundation of China (N°10434100 and N°10504037). One of the authors, L. Chen, gratefully acknowledges the support of K. C. Wong Education Foundation, Hong Kong.

References

[1] Andersen T 2004 *Phys. Rep.* **394** 157
[2] Appell J 1978 *Collision Spectroscopy* ed R G Cooks (New York: Plenum) p 227
[3] Fournier P G *et al* 1986 *Phys. Rev.* A **34** 1657
[4] Furuhashi O *et al* 2001 *Chem. Phys. Lett.* **337** 97
[5] Chen L, Martin S, Bernard J and Brédy R 2007 *Phys. Rev. Lett.* **98** 193401
[6] Martin S, Chen L, Salmoun A, Li B, Bernard J and Brédy R 2008 *Phys. Rev.* **A77** 043201
[7] Meyer F W, Yan Q, Zeijlmans van Emmichoven P, Hughes I G and Spierings G 1997 *Nucl. Instrum. Methods Phys. Res.* B **125** 138
[8] Auth C, Borisov A G and Winter H 1995 *Phys. Rev. Lett.* **75** 2292
[9] Martin S, Chen L, Bernard J, Brédy R, Buchet-Poulizac M C, Ma X and Wei B 2006 *Europhys. Lett.* **74** 985
[10] de Vries J,, Hoekstra R, Morgenstern R and Schlathölter T 2003 *Phys. Rev. Lett.* **91** 053401
[11] Deng Z, Bald I, Illenberger E and Huels M A 2006 *Phys. Rev. Lett.* **96** 243203
[12] Moretto-Capelle P, Padellec A, Brière G, Massou S and Franceries F 2007 *J. Chem. Phys.* **127** 234311
[13] Alvarado F, Bari S, Hoekstra R and Schlathölter T 2007 *J. Chem. Phys.* **127** 034301
[14] Schlathölter T, Alvarado F, Bari S, Lecointre A, Hoekstra R, Bernigaud V, Manil B, Rangama J and Huber B 2006 *Chem. Phys. Chem.* **7** 2339
[15] Brédy R *et al J. Chem. Phys.* at press
[16] Alvarado F, Bernard J, Li B, Brédy R, Chen L, Hoekstra R, Martin S and Schlathölter T 2008 *Chem. Phys. Chem.* **9** 1254
[17] Martin S, Chen L, Denis A, Bredy R, Bernard J and Désesquelles J 2000 *Phys. Rev.* A **62** 022707
[18] Jagutzki O, Mergel V, Ullmann-Pfleger K, Spielberger L, Spillmann U, Dörner R and Schmidt-Böcking H 2002 *Nucl. Instrum. Methods Phys. Res.* A **477** 244
[19] Barat M, Brenot J C, Fayeton J A and Picard Y J 2000 *Rev. Sci. Instrum.* **71** 2050
[20] Brehm B, Grosser J, Ruscheinski T and Zimmer M 1995 *Meas. Sci. Technol.* **6** 953
[21] Brédy R, Bernard J, Chen L, Wei B, Salmoun A, Bouchama T, Buchet-Poulizac M C and Martin S 2005 *Nucl. Instrum. Methods Phys. Res.* B **235** 392
[22] Cederquist H, Fardi A, Haghighat K, Langereis A, Schmidt H T and Schwartz S H 2000 *Phys. Rev.* A **61** 022712
[23] Campbell E E B, Raz T and Levine R D 1996 *Chem. Phys. Lett.* **253** 261
[24] Martin S *et al* unpublished